

Beobachten mit modernen Großteleskopen

„Zu Besuch“ beim Very Large
Telescope der ESO in Chile

Carolin Liefke

1. Dezember 2016



Der Stern CN Leo (Wolf 359)

- Von der Sonne aus gesehen der fünftnächste Stern
- Etwa so „hell“ wie Pluto ($m_V = 13.45$ mag)
- Rötliche Farbe (Spektraltyp M5.5), Oberflächentemperatur ca. 2500°C
- Zeigt Helligkeitsausbrüche (sogenannte Flares)
- Röntgenquelle

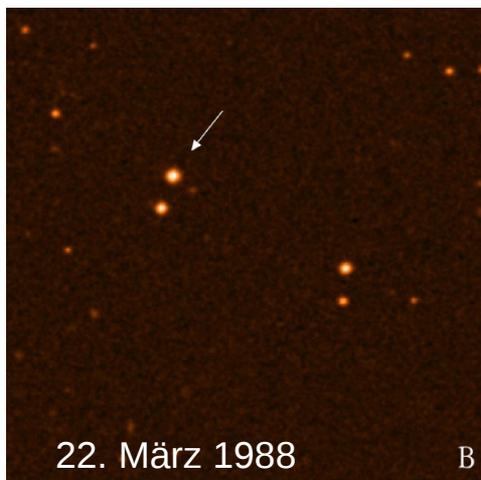


Bild: DSS2

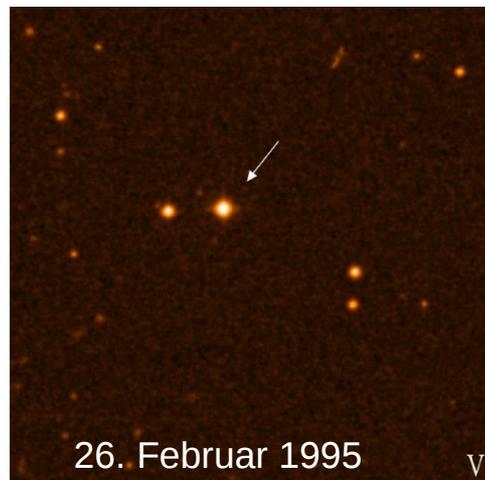
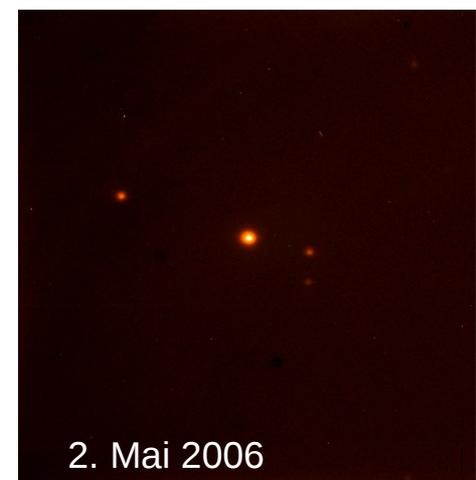


Bild: DSS2



Eigenes Bild

Lichtverschmutzung

- Moderne Großobservatorien befinden sich an abgelegenen Standorten fernab größerer Städte



Blick vom Heidelberger
Königstuhl über die
Rheinebene

Eigenes Bild

Beobachtungsanträge

Von der Idee für ein Forschungsprojekt zu den Messdaten

- Formulierung als Antrag: Welches Himmelsobjekt, Forschungsfrage, wie lange, warum mit diesem Teleskop/Instrument?
- Gutachterkomitee wählt die besten Anträge aus
- Überbuchungsfaktor bei HST, VLT etc. liegt bei 5-7



European Organisation for Astronomical Research in the Southern Hemisphere

OBSERVING PROGRAMMES OFFICE • Karl-Schwarzschild-Straße 2 • D-85748 Garching bei München • e-mail: ope@eso.org • Tel.: +49 89 320 06473

APPLICATION FOR OBSERVING TIME

PERIOD: 98A

Important Notice:

RRM ToO

By submitting this proposal, the PI takes full responsibility for the content of the proposal, in particular with regard to the names of CoIs and the agreement to act according to the ESO policy and regulations, should observing time be granted.

1. Title		Category: D-3							
Chasing stellar giant flares with UVES or X-Shooter in Rapid Response Mode									
2. Abstract / Total Time Requested									
Total Amount of Time: 0 nights VM, 4 hours SM									
We propose to observe a giant stellar flare – so strong that it triggers the BAT detector on-board the Swift satellite – immediately after the flare outburst with UVES or X-Shooter in Rapid Response Mode. Tremendous amounts of energy are released in such an extremely rare event, and optical spectroscopy will allow us to determine how the physical conditions in the lower atmosphere react to this violent change. By monitoring flare continuum emission and the fluxes and shapes of chromospheric emission lines from the UV up into the infrared, we will investigate how the flare energy is redistributed in photosphere, chromosphere, and transition region, and which processes let the stellar atmosphere return to its quiescent state.									
3. Run	Period	Instrument	Time	Month	Moon	Seeing	Sky	Mode	Type
A	98	UVES	1h	any	n	n	THN	s	TOO
B	98	XSHOOTER	1h	any	n	n	THN	s	TOO
C	98	UVES	1h	any	n	n	THN	s	TOO
D	98	XSHOOTER	1h	any	n	n	THN	s	TOO
4. Number of nights/hours				Telescope(s)		Amount of time			
a) already awarded to this project:				UT2		2h in Periods 86-90, 93 and 95, but no observations.			
b) still required to complete this project:									
5. Special remarks:									
				The RMM trigger process for the proposed observation of this very rare event will be handled automatically. A script will check alert notices from the Swift satellite for transient sources of stellar origin, check the visibility at Paranal, and send the trigger information for the observations.					
6. Principal Investigator:				Carolin Liefke, liefke@hda-hd.de, D, Zentrum fuer Astronomie					

Die chilenische Atacamawüste

- Liegt im Regenschatten der Anden, der Humboldtstrom verhindert die Bildung von Regenwolken



Luftbild des Paranal-
Observatoriums. Foto: ESO/M.
Tarenghi

Der Berg Paranal

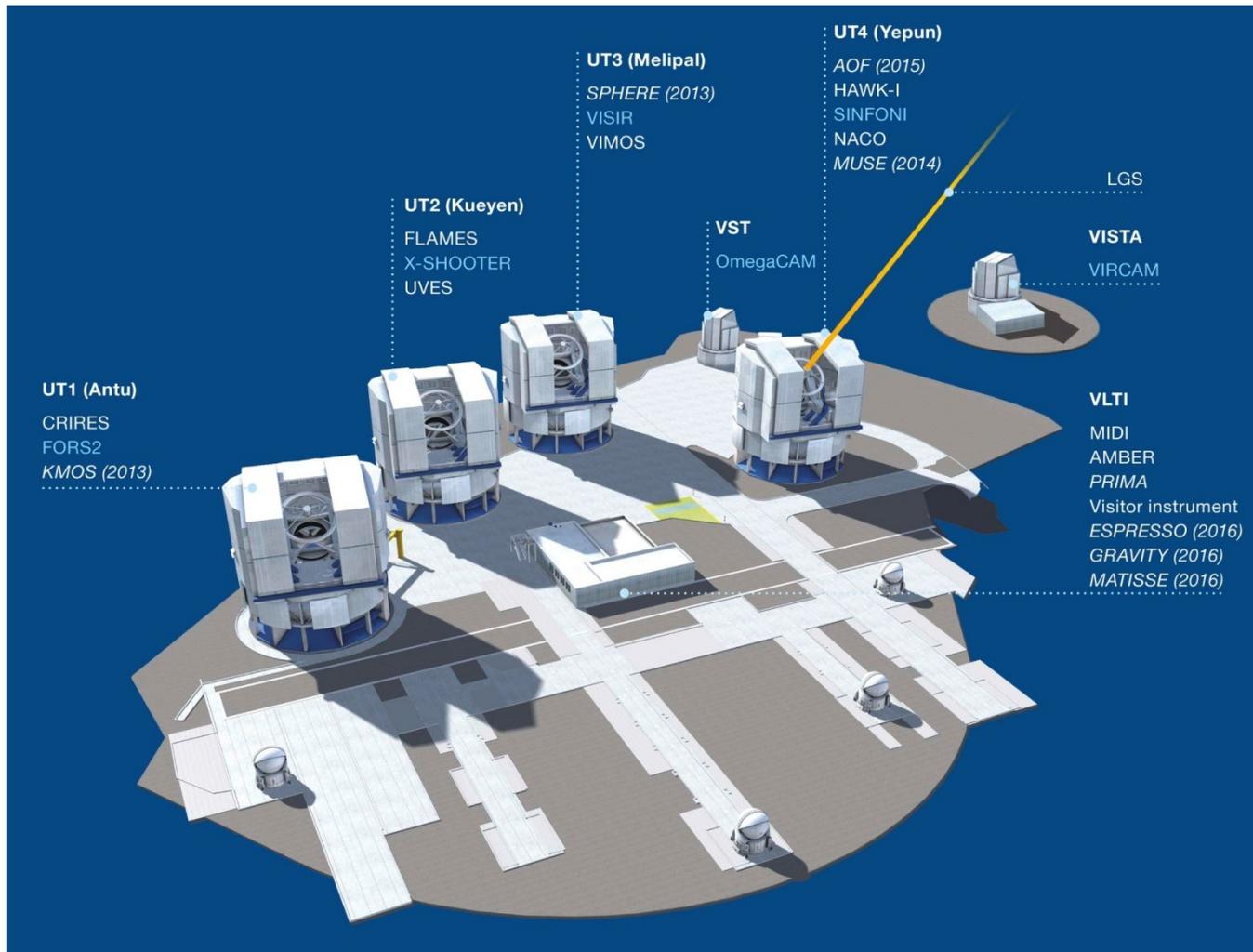
- 2635 m hoch, ca. 120 km südlich von Antofagasta und 12 km von der Pazifikküste entfernt
- Errichtung des Very Large Telescope ab Anfang der 1990er



Die vier Schutzbauten des VLT
auf der eingeebneten
Beobachtungsplattform des
Paranal

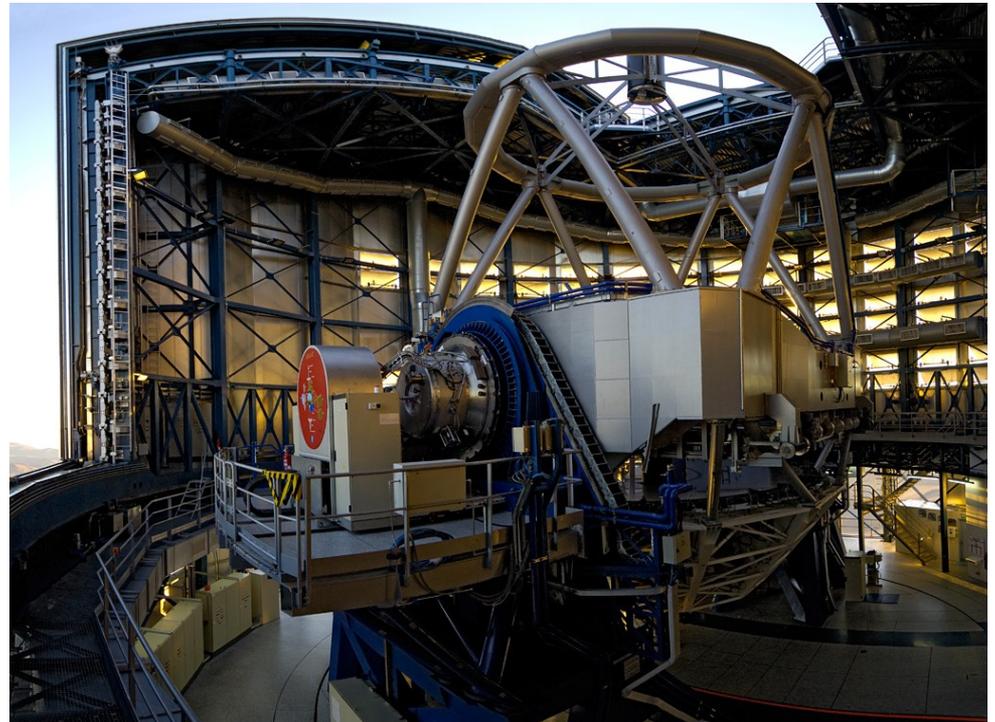
Eigenes Bild

Das Observatorium



Die VLT-Hauptteleskope

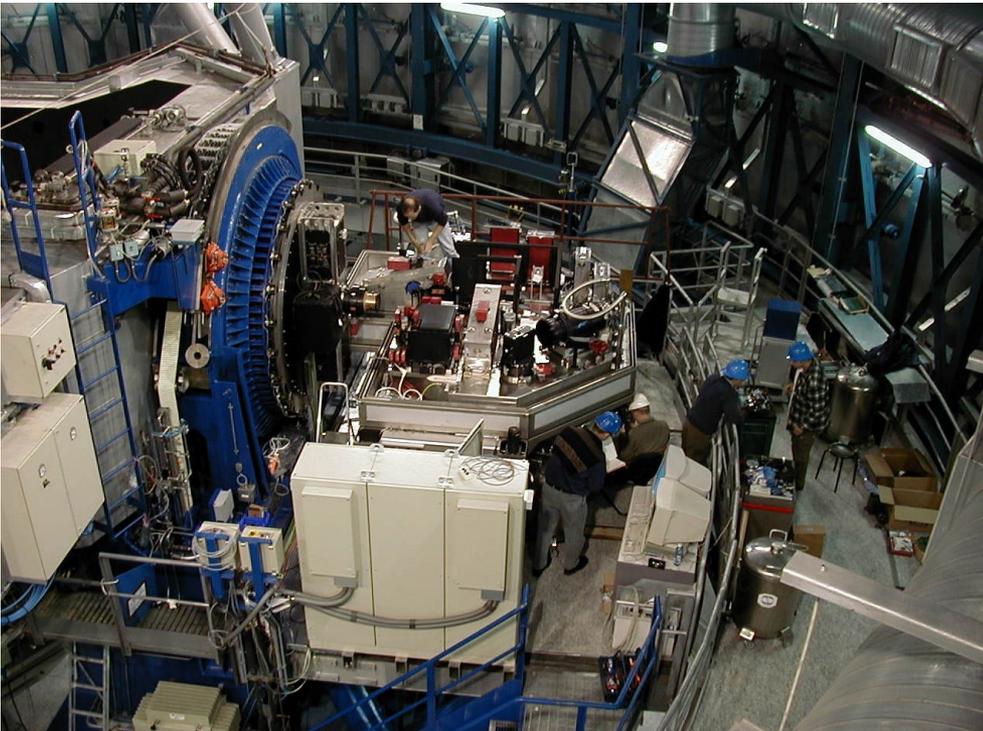
- Vier Einzelteleskope mit 8,2 Metern Spiegeldurchmesser
- Auch als Interferometer zusammenschaltbar
- Jeweils 3 Instrumente



VLT-Hauptteleskop 1. Foto: ESO

Der UVES-Spektrograf

- Spektralanalyse liefert Informationen über Temperaturen, Rotationsgeschwindigkeit, Elementhäufigkeiten, Sternflecken, Vorhandensein von Planeten...



Installation des UVES-Spektrografen im Jahr 1999. Foto: ESO

Im Kontrollzentrum



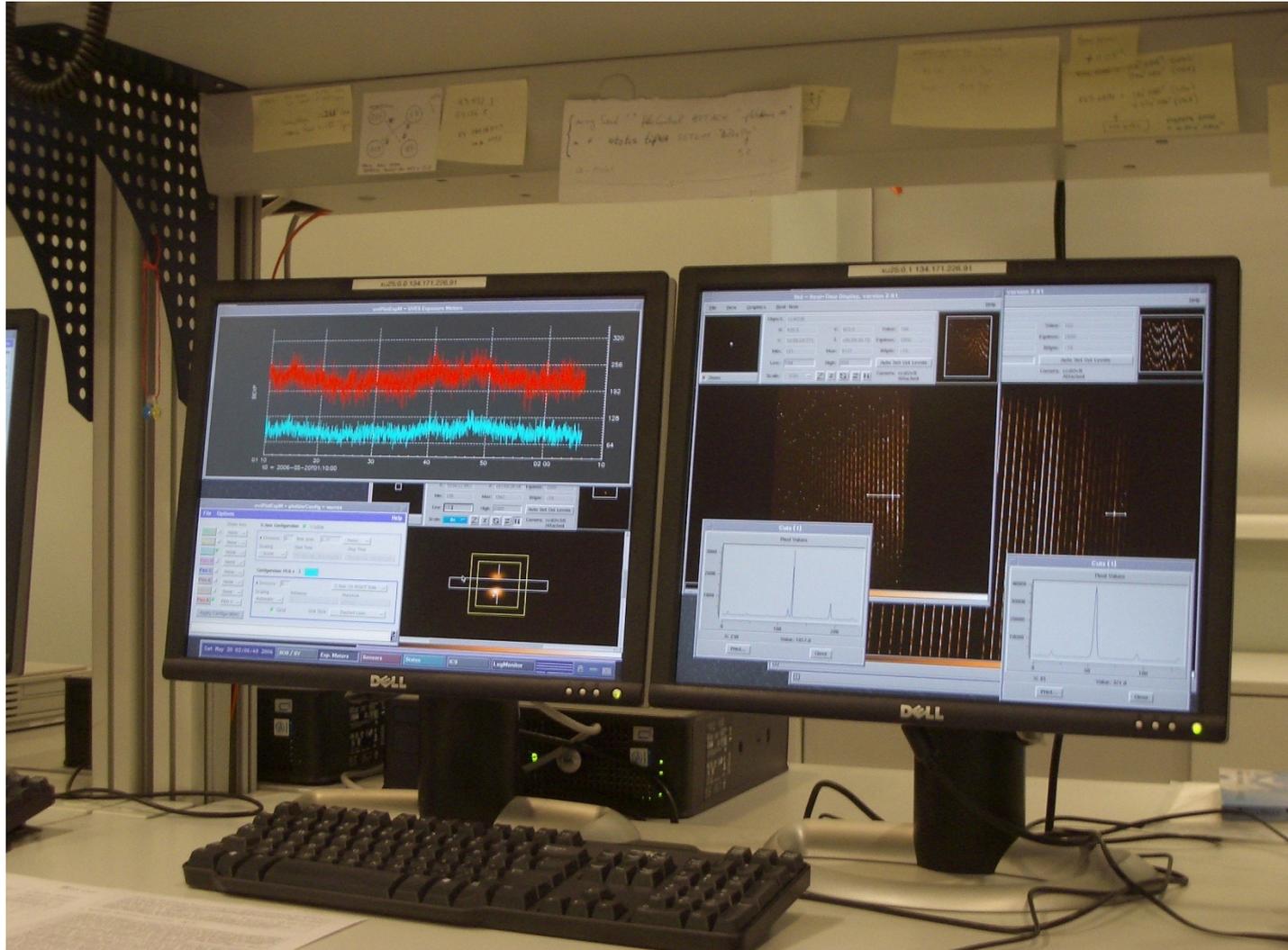
Bild: ESO

Bei der Arbeit...



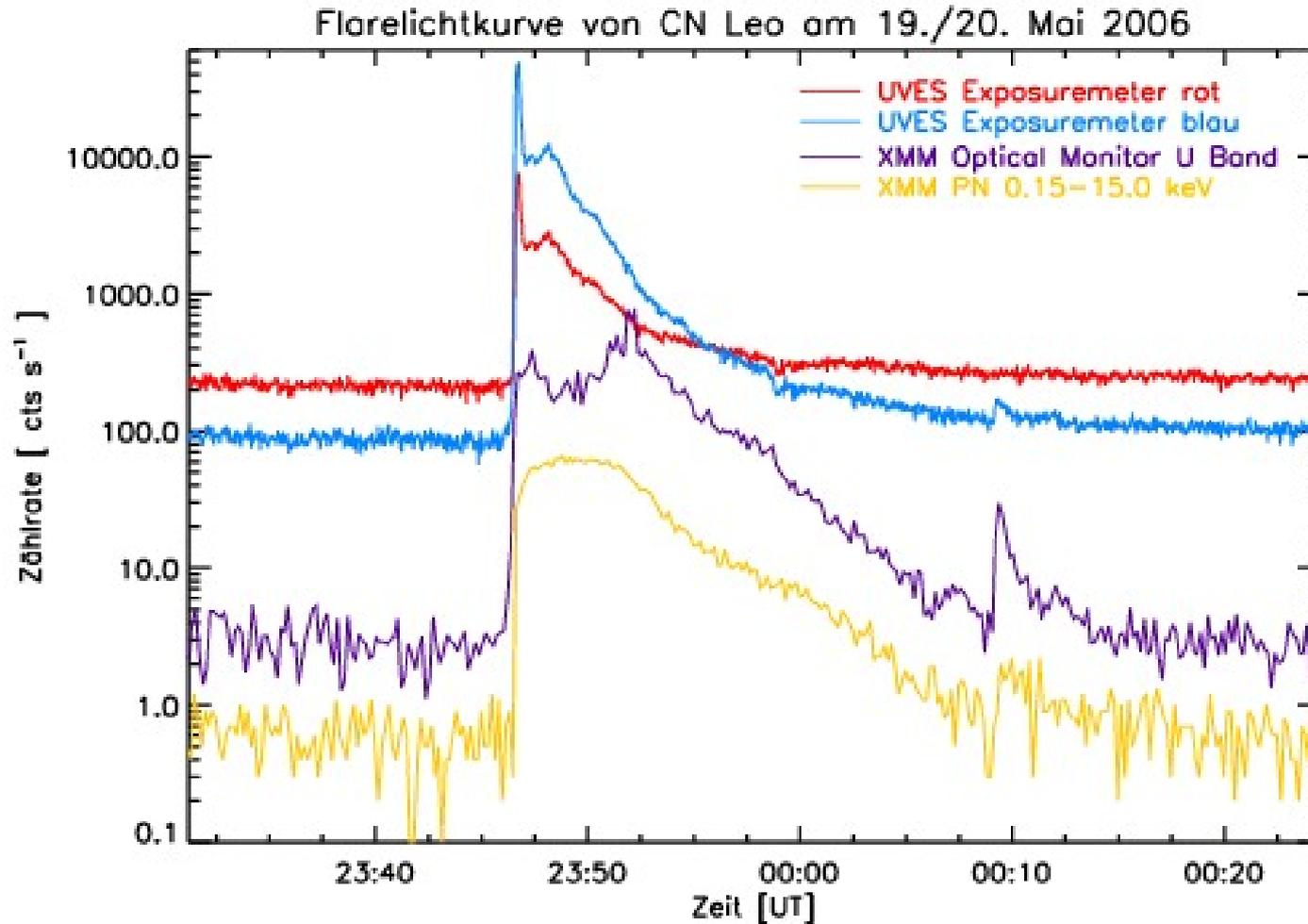
Bild: ESO/H.H.Heyer

CN Leo fest im Blick

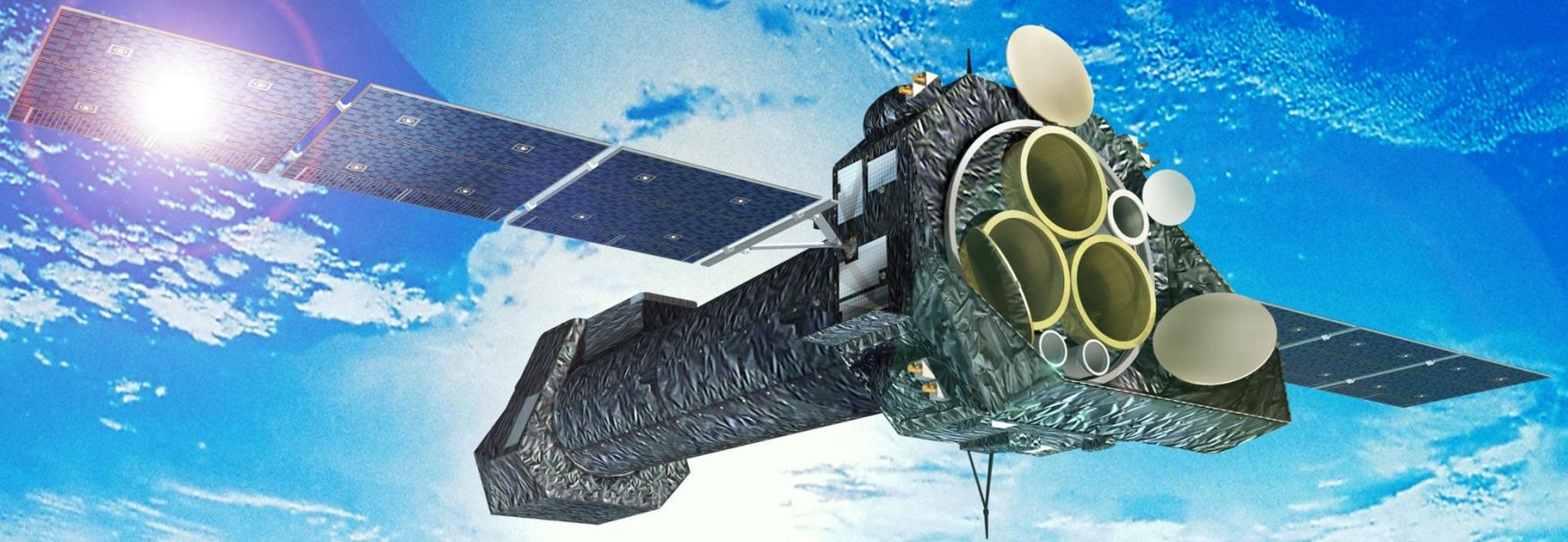


Eigenes Bild

Ein Helligkeitsausbruch...



Röntgensatellit XMM-Newton

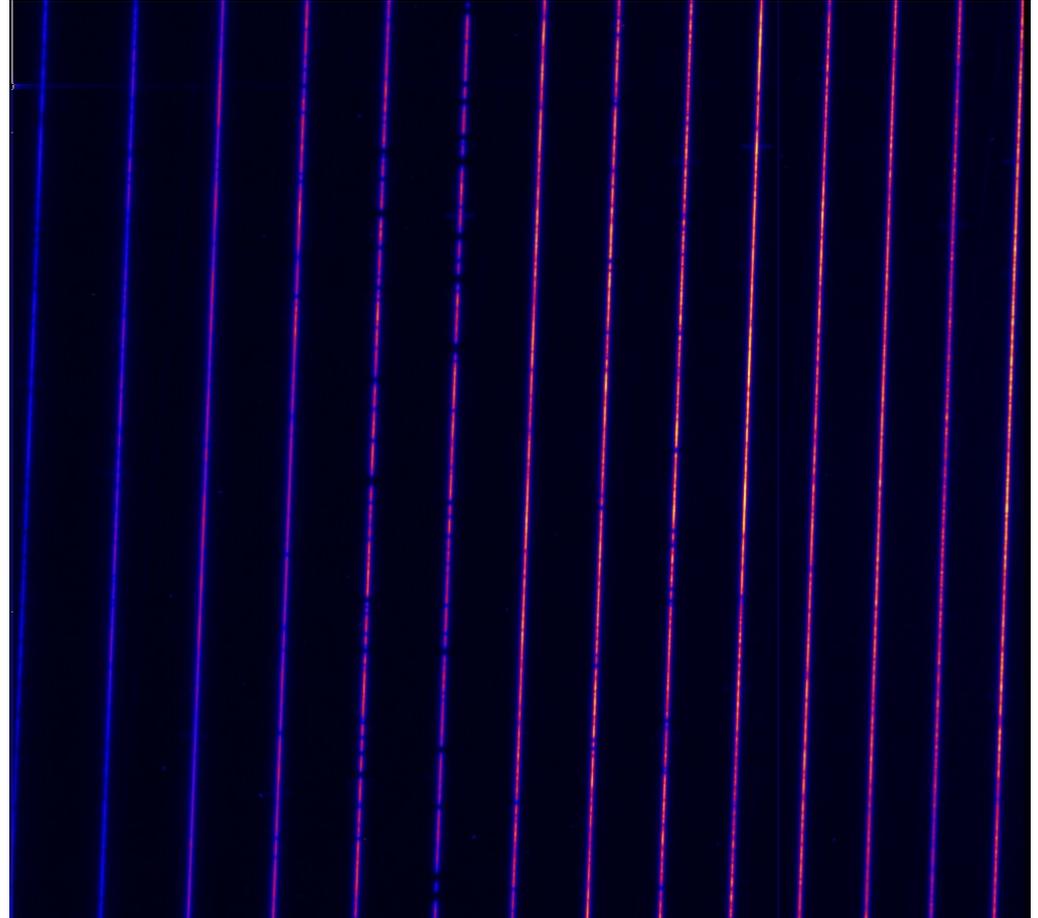


Datenreduktion

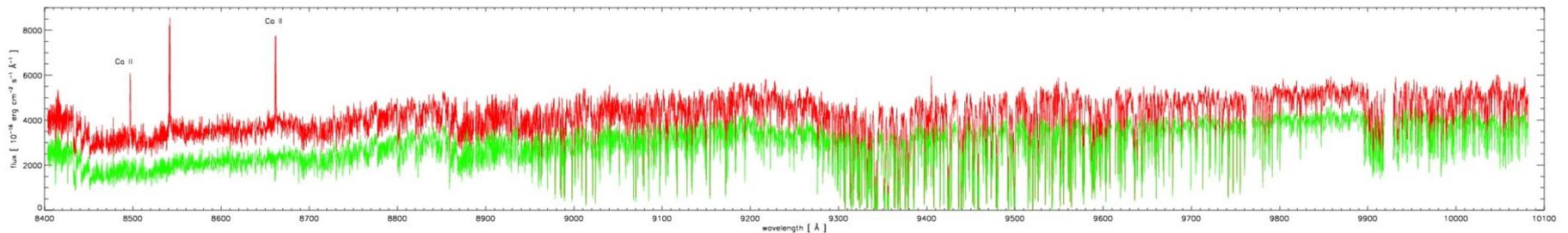
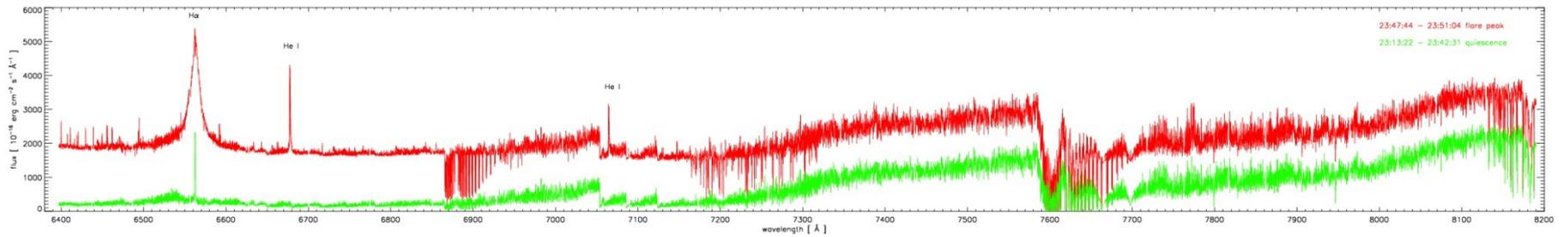
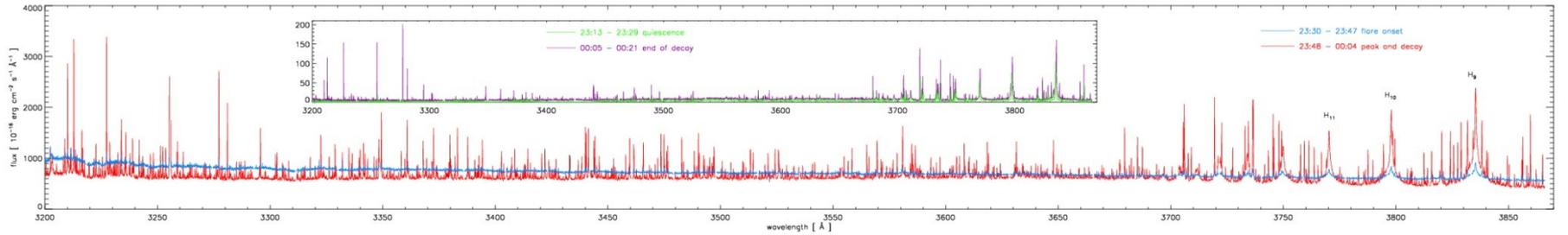
Auch bei Spektren:

- Bias und Flatfield
- Korrektur von Cosmics, Bad Pixeln und Dead/Hot Columns

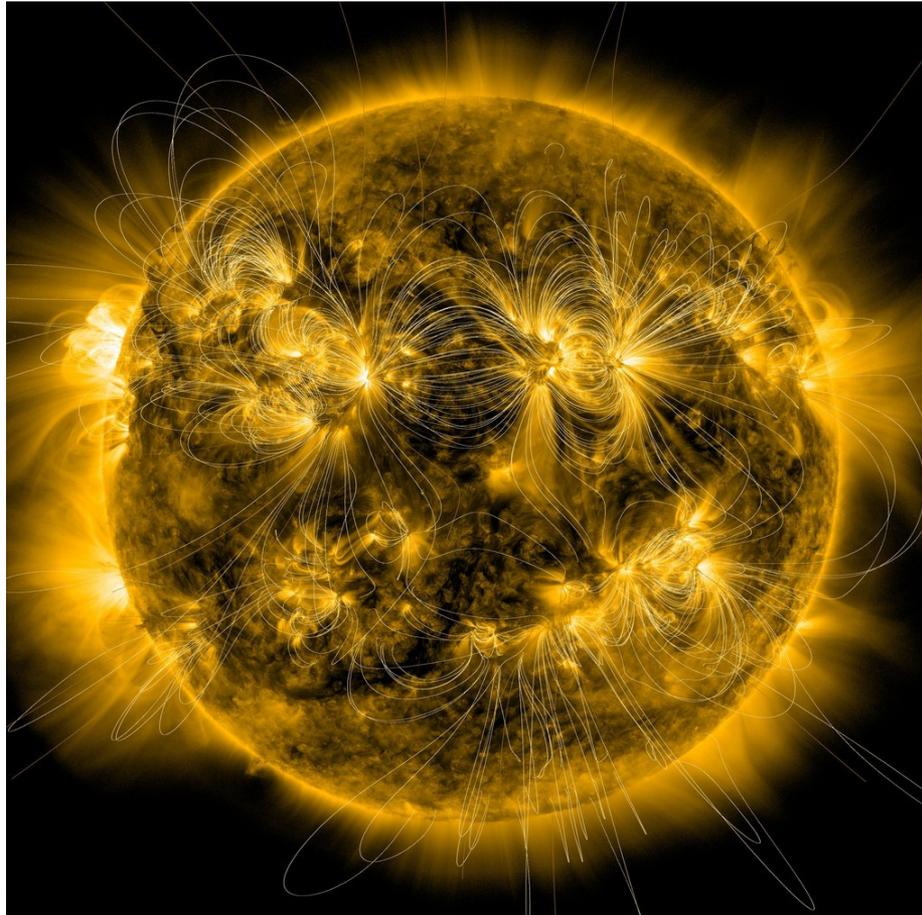
- Sternspektren und Himmelshintergrund extrahieren
- Flußkalibration (Standardstern)



... und deren Ergebnisse



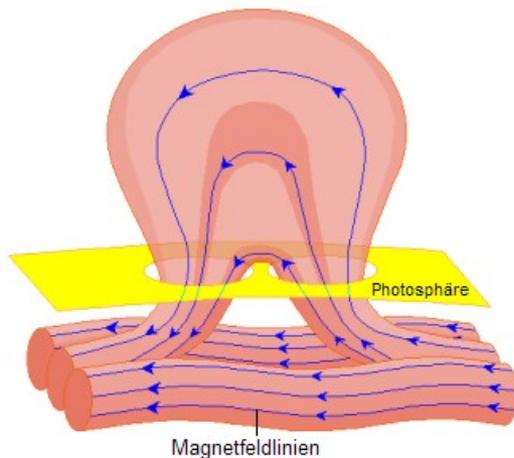
Knoten in Magnetfeldern



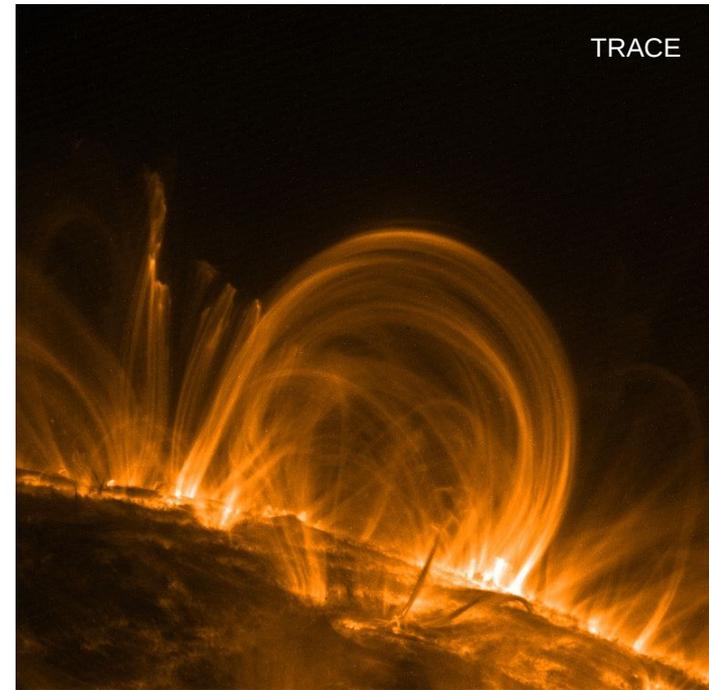
SDO AIA 171 Å Röntgenaufnahme der Sonnenkorona mit rekonstruierten Magnetfeldlinien. Bild: NASA/SDO and the AIA and HMI science teams

Koronale Bögen

- Bögen über Flecken/aktiven Regionen
- Arkaden: Anordnungen von Bögen
- Veränderungen innerhalb von Minuten
 - Neue Bogenverbindungen
 - Wachstum von Arkaden



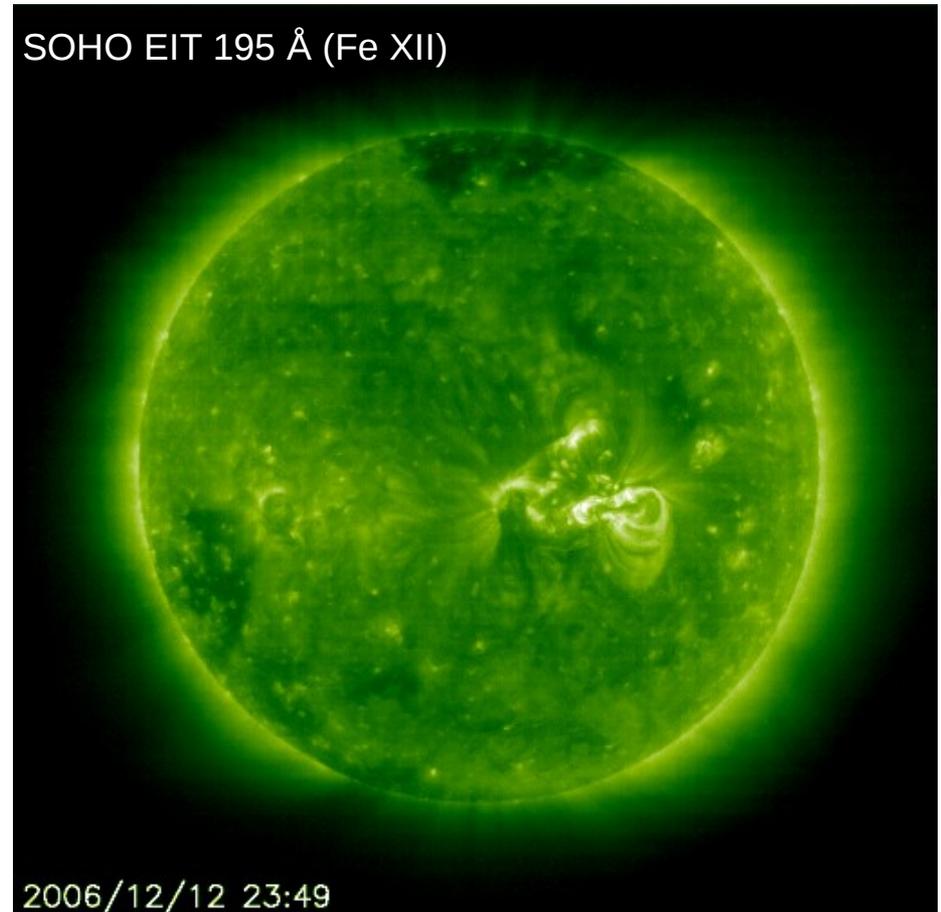
Benutzer Lmb via Wikimedia Commons (Public Domain)



- Magnetische Flußröhren: Geladene Plasmateilchen folgen Magnetfeldern
- Streamer: offene Magnetfeldlinien

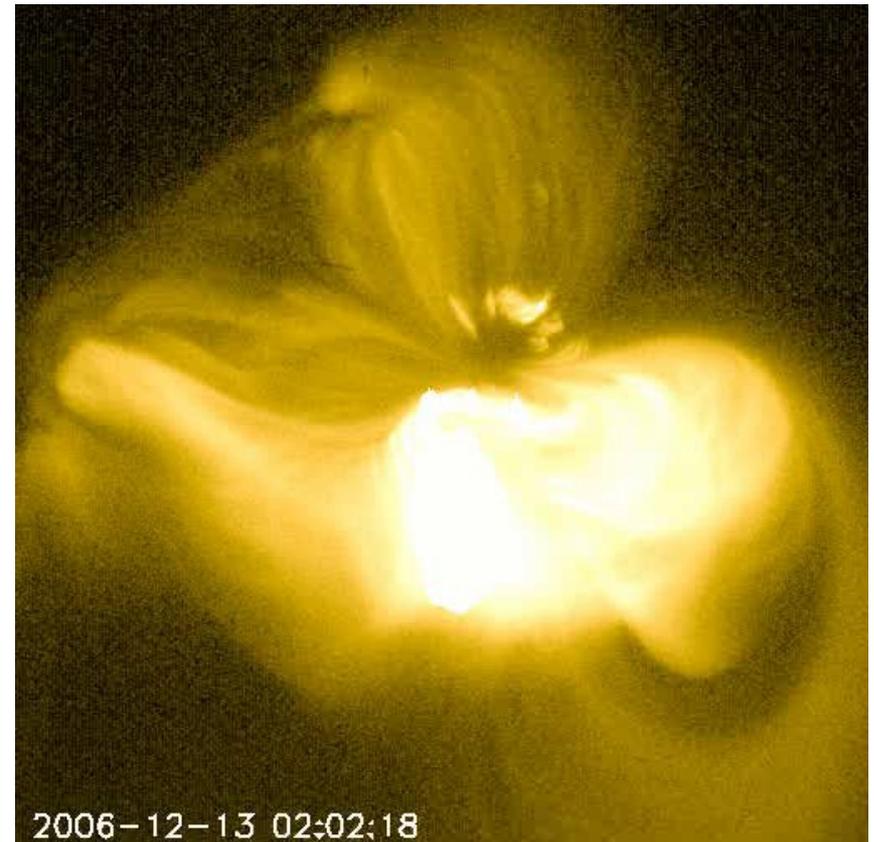
Flares auf der Sonne

- „Magnetische Rekonnektion“ in der Korona
- Beschleunigte Teilchen treffen auf die unteren Atmosphären- schichten und heizen sie auf
- Abkühlung durch Aussendung von Strahlung: Linienemission und Kontinuum
- „Chromosphärische Evaporation“ trägt frisches Material in die Korona, das Röntgenstrahlung aussendet



Flares auf der Sonne

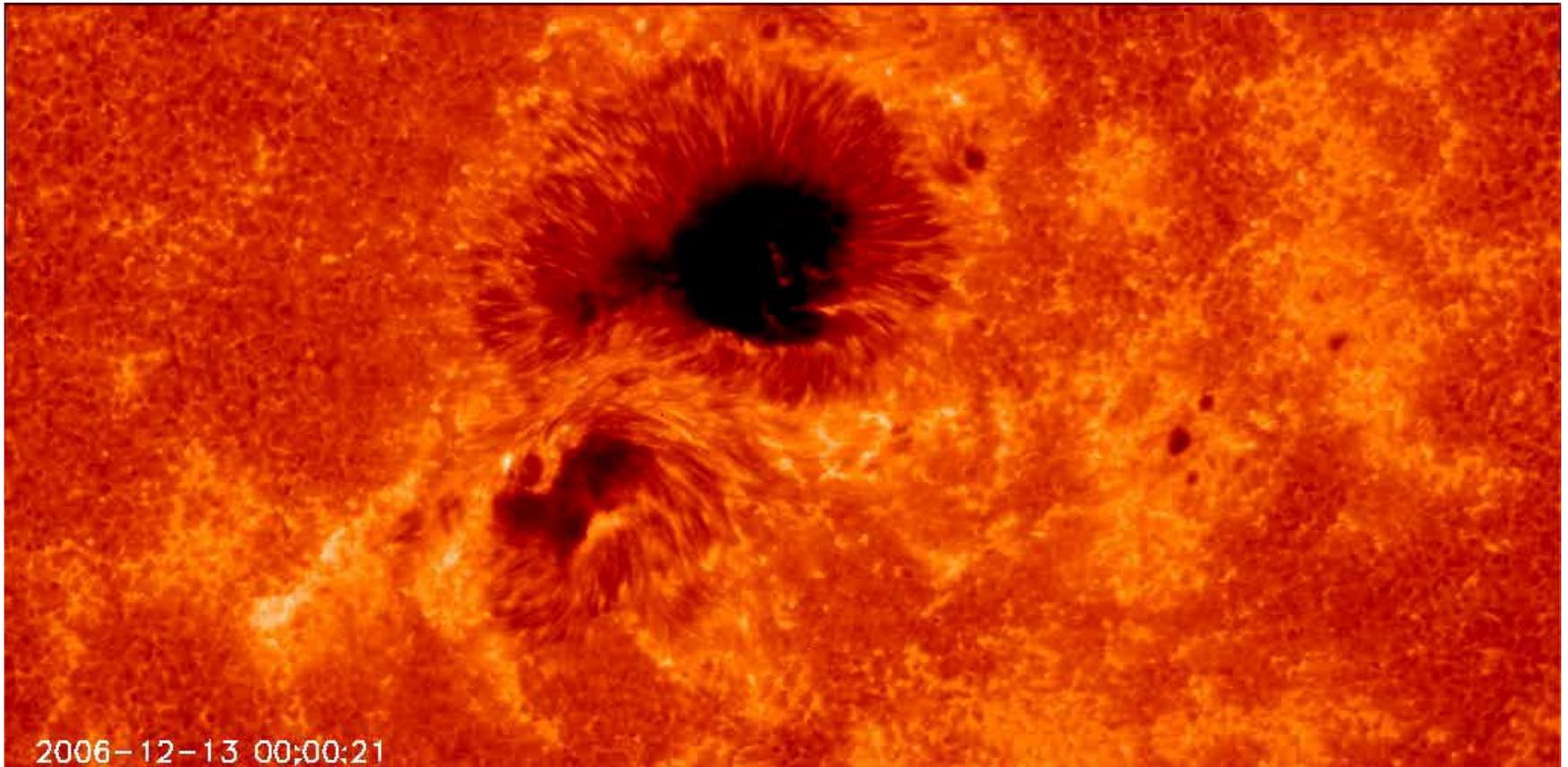
- „Magnetische Rekonnektion“ in der Korona
- Beschleunigte Teilchen treffen auf die unteren Atmosphärenschichten und heizen sie auf
- Abkühlung durch Aussendung von Strahlung: Linienemission und Kontinuum
- „Chromosphärische Evaporation“ trägt frisches Material in die Korona, das Röntgenstrahlung aussendet



Hinode XRT

Flares auf der Sonne

Hinode SOT



Resultate

- Eigenschaften des Flare-Plasmas: Änderungen von koronale Temperaturen und Dichten, chromosphärischen Dichten, Elementhäufigkeiten
- Aussehen der Flareregion: Länge des koronalen Bogens, Querschnittsfläche in der Photosphäre, Aufheizen der Sternoberfläche
- Auf- und Abbewegungen von Materie
- Möglicherweise Veränderungen im Magnetfeld des Sterns in Zusammenhang mit dem Flare
- ...

Konferenzen I

- Aktuelle Forschungsergebnisse werden auf (internationalen) Fachtagungen vorgestellt
- Alle zwei Jahre findet die Konferenz „Cool Stars, Stellar Systems, and the Sun“ statt, zum Beispiel 2006 in Pasadena, 2008 in St. Andrews und 2010 in Seattle



The many faces of a giant flare

Multiwavelength observations of CN Leo with high spectral and high time resolution

CAROLIN LEHRKE and JURGEN H. M. M. SCHMITT
Hamburger Sternwarte, Universitaet Hamburg
e-mail: cllehrke@hamburger.de

Abstract

The MS star CN Leo has been observed simultaneously with XMM-Newton and X-IFU on 1920 May 2006. A giant flare occurred at 21:47 UT on 19 May and is covered in detail by instruments. This study reports on the multiwavelength observations of the flare. The flare is observed in X-ray, in the UV band by the optical filter, and by X-IFU. The optical filter observations show the development of the flare in the UV band. The X-IFU observations show the development of the flare in the X-ray band. The flare is observed in X-ray, in the UV band by the optical filter, and by X-IFU. The optical filter observations show the development of the flare in the UV band. The X-IFU observations show the development of the flare in the X-ray band.

Lightcurves

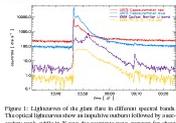


Figure 1: Lightcurves of the flare in different spectral bands. The plot shows flux versus time for various filters: X-IFU (red), X-IFU (green), X-IFU (blue), X-IFU (purple), X-IFU (orange), X-IFU (yellow), X-IFU (cyan), X-IFU (magenta), X-IFU (brown), X-IFU (pink), X-IFU (grey).

EPIC spectra

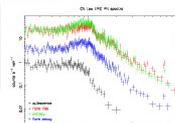


Figure 2: EPIC spectra covering the full phase of the flare. The plot shows flux versus energy for different spectral bands: X-IFU (red), X-IFU (green), X-IFU (blue), X-IFU (purple), X-IFU (orange), X-IFU (yellow), X-IFU (cyan), X-IFU (magenta), X-IFU (brown), X-IFU (pink), X-IFU (grey).

Coronal densities

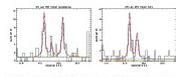


Figure 4: Core spectra in X-IFU during quiescence and flare. The plot shows flux versus energy for different spectral bands: X-IFU (red), X-IFU (green), X-IFU (blue), X-IFU (purple), X-IFU (orange), X-IFU (yellow), X-IFU (cyan), X-IFU (magenta), X-IFU (brown), X-IFU (pink), X-IFU (grey).

Chromospheric lines

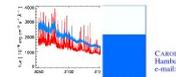


Figure 5: Continuum observations of the flare in the optical band. The plot shows flux versus wavelength for different spectral bands: X-IFU (red), X-IFU (green), X-IFU (blue), X-IFU (purple), X-IFU (orange), X-IFU (yellow), X-IFU (cyan), X-IFU (magenta), X-IFU (brown), X-IFU (pink), X-IFU (grey).

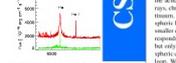


Figure 6: Evolution of the flare in the optical band. The plot shows flux versus wavelength for different spectral bands: X-IFU (red), X-IFU (green), X-IFU (blue), X-IFU (purple), X-IFU (orange), X-IFU (yellow), X-IFU (cyan), X-IFU (magenta), X-IFU (brown), X-IFU (pink), X-IFU (grey).

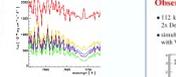


Figure 7: Evolution of individual flare loops. The plot shows flux versus wavelength for different spectral bands: X-IFU (red), X-IFU (green), X-IFU (blue), X-IFU (purple), X-IFU (orange), X-IFU (yellow), X-IFU (cyan), X-IFU (magenta), X-IFU (brown), X-IFU (pink), X-IFU (grey).

The CN Leo flare census

CAROLIN LEHRKE, BIRGIT FUBENSTEIN, and JURGEN H. M. M. SCHMITT
Hamburger Sternwarte, Universitaet Hamburg
e-mail: cllehrke@hamburger.de

Abstract

We investigate the frequency and amplitude distribution of flares on the active M dwarf CN Leo observed simultaneously in coronal X-rays, chromospheric line emission, and the photospheric optical continuum. We find that most of the large flares are visible in all atmospheric layers, there are equivalent to solar light flares. Several smaller events are only visible in the chromospheric lines, which we compare to solar H-alpha flares. One event is very strong in X-rays, but only weak in the chromospheric lines and invisible in the photospheric continuum, indicating a rather large scale height of the flare loop. We find no obvious correlation of the flare amplitude and decay times in the different atmospheric layers. We also search for time lags between the different wavelength bands and probe the occurrence of the Neupert effect.

Observations

• 112 ks of data in six XMM-Newton observations (1x May 2004, 2x December 2005, 3x May 2006)
• simultaneous optical photometry and high-resolution spectroscopy with VEPIC/ES

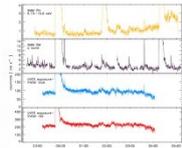


Figure 1: Multiband photometry of CN Leo, 1920 May 2006. The plot shows flux versus time for various filters: X-IFU (red), X-IFU (green), X-IFU (blue), X-IFU (purple), X-IFU (orange), X-IFU (yellow), X-IFU (cyan), X-IFU (magenta), X-IFU (brown), X-IFU (pink), X-IFU (grey).

Three large flares in X-rays in the observation on 1920 May 2006.
• A giant flare at 1:47 UT (Schmitt et al. 2006; Fubenstein et al. 2006; Lehrke et al. in preparation)
• A second strong event at 1:45 shows an unusually symmetric X-ray lightcurve with a rather slightly longer than the decay (see Fig. 4b) and exhibits comparably weak signatures of optical wavelengths, indicating that the flare does not penetrate down to the lower layers of the stellar atmosphere.
• A third strong flare is simultaneously observed by the UVER data any more.

Flare statistics

Most of the 27 flares observed during the six observations are of short duration (< 3 hours in X-rays, optical filter duration are even shorter). In Fig. 2 we search for dependencies of the exponential decay times and the times from the optical filter to the blue optical band, the U band, and in X-rays.

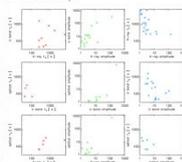


Figure 2: Correlations of flare decay times (left row) and asymptotic second time in different spectral bands, and decay times vs. asymptotic second time. The plot shows flux versus time for various filters: X-IFU (red), X-IFU (green), X-IFU (blue), X-IFU (purple), X-IFU (orange), X-IFU (yellow), X-IFU (cyan), X-IFU (magenta), X-IFU (brown), X-IFU (pink), X-IFU (grey).

Flare evolution and loop half lengths

Only the three large X-ray flares on May 1920 May 2006 allow resolved spectroscopy. Fig. 3 shows the evolution of emission-measured temperature and total emission measure of 2 temperature-resolved EPIC models.

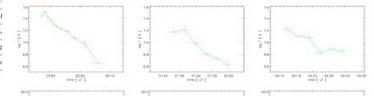


Figure 3: Temporal evolution of flare temperature (left row) and total emission measure (second row), and density temperature phase (left row) for the giant flare (left column), the 'symmetric' flare at 1:47 UT (middle column), and the flare at 1:15 UT (right column). The plot shows flux versus time for various filters: X-IFU (red), X-IFU (green), X-IFU (blue), X-IFU (purple), X-IFU (orange), X-IFU (yellow), X-IFU (cyan), X-IFU (magenta), X-IFU (brown), X-IFU (pink), X-IFU (grey).

With $\chi^2/\text{d.o.f.}$ as a proxy for α , the flare decay can be fitted with a linear slope in the density temperature phase according to Reale (2007) in order to obtain an estimate of the half length of the flaring loop. The resulting loop half lengths for the three flare events are all ~ 10000 km, comparable to coronal loops on the Sun but corresponding to $\sim 1/10 - 1/15$ of the stellar radius for CN Leo. The fact that very similar loop lengths are obtained for the three flare events indicate that they have their origins in the same loop.

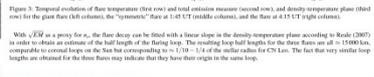


Figure 4: U band and X-ray lightcurves together with the first derivative of the X-ray data for the giant flare (left), the 'symmetric' flare (middle) and the flare at 1:15 UT (right). The plot shows flux versus time for various filters: X-IFU (red), X-IFU (green), X-IFU (blue), X-IFU (purple), X-IFU (orange), X-IFU (yellow), X-IFU (cyan), X-IFU (magenta), X-IFU (brown), X-IFU (pink), X-IFU (grey).

For the three strong X-ray flares on a 1920 May 2006, we test the Neupert effect relative to the time integral of the hard X-ray flux being proportional to the soft X-ray flux. We use the U band emission, which contains mainly of continuum emission (free chromospheric line emission which is supposed to be excited instantaneously by the accelerated electrons which cause also the softest hard X-rays, as a proxy. Fig. 4 shows the time derivatives of the X-ray lightcurve together with the U band lightcurve. Only for the third flare event at 1:15 UT the Neupert relation holds.

Conclusions

- We observe 27 flares on the MS star CN Leo in 112 ks of X-ray data and six half hours of nearly simultaneous optical spectroscopy and photometry (10 ks in X-rays, 17 ks in U band, 10 ks in the optical blue band)
- Average flare duration are 28 minutes in X-rays, 325 seconds in the U band, and 100 seconds in the optical blue band
- The flare decay times and amplitudes in the different spectral bands do not show strong correlations
- The final cooling loop lengths amount 10000 km for three major flares occurring within 6 hours, suggesting that the events originate from the same loop
- Flare observations do not seem to show delays in the onset of optical, U band, and X-ray emission
- The Neupert effect is only visible for the last of the three large flares

References

Fubenstein, B., Löffler, C., A. Schmitt, J. H. M. M., 2007, A&A, 468, 221
Fubenstein, B., Löffler, C., Schmitt, J. H. M. M., & Retner, A. 2008, A&A, in press
Lehrke, C., Fubenstein, B., A. Schmitt, J. H. M. M., 2006, A&A, 471, 271
Schmitt, J. H. M. M., Reale, T., Löffler, C., et al. 2008, A&A, 481, 799

Konferenzen II

- Kleine Workshops bis hin zu internationalen Veranstaltungen mit mehreren 100 Teilnehmern
- Vorträge im Plenum
- Poster mit neuesten Forschungsergebnissen
- „Splinter Meetings“
- Allgemeiner Informationsaustausch

...

Multiwavelength observations of a giant flare on CN Leonis*

III. Temporal evolution of coronal properties

C. Lielke^{1,2}, B. Fuhrmeister¹, and J. H. M. Schmitt¹

¹ Hamburger Sternwarte, Universität Hamburg, Gojenbergsweg 112, 21029 Hamburg, Germany
e-mail: c.lielke@hs.uni-hamburg.de
² Zentrum für Astronomie, Mönchhofstraße 12-14, 69120 Heidelberg, Germany
Received 7 January 2010 / Accepted 11 March 2010

ABSTRACT

Coronal X-ray flares affect all atmospheric layers from the photosphere over chromosphere and transition region up into the corona. Simultaneous observations in different spectral bands allow to obtain a comprehensive picture of the environmental conditions and the physical processes going on during different phases of the flare. We investigate the properties of the coronal plasma during a giant flare on active M-dwarf CN Leo observed simultaneously with the UVES spectrograph at Keck II and XMM-Newton. From one optical flare, we analyze the temporal evolution of the coronal temperature and emission measure, and investigate variations in electron density and coronal abundances during the flare. Optical Fe XIII line emission traces the cooler quietest coronal levels. Although of rather short duration (exponential decay time $\tau_{\text{dec}} \approx 5$ min), the X-ray flux in this flare peak exceeds the quiescent level by a factor of ≈ 10 . The electron density averaged over the whole flare is greater than $5 \times 10^{17} \text{ cm}^{-3}$. The flare plasma shows an enhancement of iron by a factor of ≈ 2 during the rise and peak phase of the flare. We derive a size of ≈ 9000 km for the flaring structure from the evolution of the emitting plasma during flare rise, peak, and decay. Conclusions: The characteristics of the flare plasma suggest that the flare originates from a compact reconnection instead of a single loop. The combined results from X-ray and optical data further constrain the plasma properties and the geometry of the flaring structure in different atmospheric layers.

1. Introduction

Flares on the Sun and on stars show a wide variety of amplitudes, from the smallest microflares to giant flares with luminosity increases by orders of magnitude, and timescales ranging from a few seconds up to several days. Depending on energy budget, decay time and shape of the lightcurve, impulsive and gradual flares can be distinguished. On the Sun, the former have been associated with compact emission regions, i.e., single loops, while the latter typically involve a series of eruptions in a whole arch of loops (so-called two-ribbon flares, see Filippov et al. 1977). For stellar flares, the loop geometry can usually not be observed directly, but scaling laws based on the hydrostatic case, relating the loop temperature and pressure with the size of the loop, as derived and tested for the quiet Sun (Rosner et al. 1978) can be adapted to stellar flares to give an estimate of the dimensions of the involved coronal structures (Achewson et al. 2010). Additionally, hydrodynamic loop modeling approaches allow to assess the loop length from the analysis of the decay of the flare in X-rays and to estimate the amount of additional heating (Sriv et al. 1991; Reale et al. 1997). This approach has recently been extended to an analysis of the rise phase of the flare (Reale 2007). Individual flare events can thus be characterized with respect to the physical properties of the flaring structure from observational quantities also available for stellar events. The greater the spectral coverage and the better the spectral and temporal resolution, the more information can be gained and the better one can constrain on the physical properties of the flare plasma and the geometry of the flaring structure. Simultaneous observations in

* Based on observations collected at the European Southern Observatory, Paranal, Chile, 07/12-01/01/10 and on observations obtained with XMM-Newton, an ESA science mission with instruments and contributions directly funded by ESA Member States and NASA.

Article published by EDP Sciences

Page 1 of 13

Multiwavelength observations of

I. The chromosphere as a

B. Fuhrmeister¹, C. Lielke^{1,2}, J. H. M.

¹ Hamburger Sternwarte, Universität Hamburg, Gojenbergsweg 112, 21029 Hamburg, Germany
e-mail: fuhrmeister@hs.uni-hamburg.de
² Universität zu Köln, Friedrich-Hülsmann-Platz 1, 53075 Köln, Germany
Received 10 January 2008 / Accepted 27 April 2008

ABSTRACT

Active stars on the main sequence exhibit a wide range of coronal temperatures and emission measures. While the coronal properties of these stars are studied best in X-ray observations, their chromospheres are investigated in the optical and infrared. We analyze simultaneous observations with UVES and XMM-Newton of a major flare on the active M-dwarf star CN Leo. The optical data cover the wavelength range from 3500 to 8500 Å. The X-ray data cover the energy range from 0.1 to 10 keV. We find that the flare is associated with a significant increase in the emission measure of the chromosphere. This increase is observed in the H α and H β lines, and in the H γ and H δ lines. The flare is associated with a significant increase in the emission measure of the chromosphere. This increase is observed in the H α and H β lines, and in the H γ and H δ lines. The flare is associated with a significant increase in the emission measure of the chromosphere. This increase is observed in the H α and H β lines, and in the H γ and H δ lines.

1. Introduction

Flaring is a commonly observed phenomenon on late-type stars. During a flare event, large amounts of energy are released probably from magnetic field reconfigurations and emitted over a wide range of the electromagnetic spectrum. Although white light flares are relatively rare for the Sun, they are quite common among M-dwarf stars, because of their lower photospheric background emission in the optical. Chromospheric emission lines trace sensitivity to flares in amplitude, line width, line shape, and wavelength shifts. In addition, optical flares often have X-ray counterparts, although there is an one-to-one relationship between X-ray and optical flares. During large flares, M-dwarf stars can show an increase in X-ray luminosity by factors up to 100 (e.g. Gidel et al. 2002, 2004), and even greater magnitude increases have occasionally been reported in the optical (e.g. Mason et al. 1992; Lawler & Pettersen 1993).

The thermal properties of the coronal flare plasma can be diagnosed from the emitted soft X-ray emission, while gyroresynchrotron radio and microwave emission typically traces nonthermal particles in the corona. Additionally, emission lines

are important for our understanding of solar and stellar flare and of coronal heating (Koslowski & Pikelner 1974; Semov et al. 1981; Torres et al. 1986; Fisher 1987; a Popular Preprint (Klimchuk 2000; Parker 1988) even attributes all of the region energy input to the quiescent solar corona to (nano-)flare input. Solar and stellar flares are observed to occur over nearly all recent time scales, ranging from a few seconds (Vilmer et al. 1994; Schmitt et al. 1995) to more than a week (Kleinman-Schmitt 1996), and the response of the heated plasma happens essentially on the mode of energy input. Thus these processes involve plasma diffusing in temperature and density more than four orders of magnitude, spanning on short and temporal scales, simultaneous multiwavelength data are sufficient to provide coverage and sufficient spectral and short arc resolution are required for any reliable observational conclusions. Since the primary energy source and energy loss process of a flare is coronal, space-based X-ray observations

Article published by EDP Sciences

Article published by EDP Sciences

Based on observations collected at the European Southern Observatory, Paranal, Chile, 07/12-01/01/10 and on observations obtained with XMM-Newton, an ESA science mission with instruments and contributions directly funded by ESA Member States and NASA.

* Main-Content International Ongoing Follow-up.

A coronal explosion o

J. H. M. Schmitt¹, F. Reale², C. Lielke¹, U.

¹ Hamburger Sternwarte, Gojenbergsweg 112, 21029 Hamburg, Germany
e-mail: jschmitt@hs.uni-hamburg.de
² Dipartimento di Scienze Fisiche e Astronomiche, Università degli Studi di Napoli, Via Cintia, 80131 Napoli, Italy
Received 7 November 2007 / Accepted 24 January 2008

LETTER TO THE EDITOR

AKA 466, 113-114 (2007)
DOI: 10.1051/0004-6461/2007395
© ESO 2007

Rapid magnetic flux variability

A. Reiners^{1,2}, J. H. M. M.

¹ Hamburger Sternwarte, Gojenbergsweg 112, 21029 Hamburg, Germany
e-mail: reiners@hs.uni-hamburg.de
² Universität zu Köln, Friedrich-Hülsmann-Platz 1, 53075 Köln, Germany
Received 15 January 2007 / Accepted 28 February 2007

ABSTRACT

We present UVES/UVI observations of the nearby flare star CN Leo. Our observations, covering three nights separated by $\Delta t = 2.2$ d. The differential data measurements show a night-to-night variability in the magnetic flux variability in time scales less

1. Introduction

The strong activity observed in many stars implies strong magnetic fields, which are thought to lie at the root of all observed activity phenomena. Yet the direct measurement of magnetic fields in stellar photospheres is difficult. Most of the methods to measure magnetic fields require the detection of Zeeman broadening in magnetically sensitive spectral lines. Magnetic field strengths up to several kG-Gauss and large filling factors have been measured for a few early M-dwarfs and T Tauri stars from optical FeI and Infrared TiI lines (for an overview see Johns-Kraft & Valenti 2004). Spectropolarimetry allows to reconstruct the field geometry for some of these objects (Donati et al. 2006). However, appropriate atomic lines for such measurements either disappear or become more and more blended with molecular lines for objects later than spectral type and M. Reiners & Reale (2006) introduced a method to measure the mean magnetic field of these otherwise short-lived lines of the FeII absorption band around 5000 Å. The FeII band comprises a large number of absorption lines with very different Zeeman sensitivities. Lines with small sensitivity can be used to determine the rotation velocity, and magnetically sensitive lines (nonzero g -factor) indicate the quality magnetic field strength \times filling factor (B_l). Reiners & Reale (2007) successfully measured the mean

AKA 466, 113-114 (2007)
DOI: 10.1051/0004-6461/2007395
© ESO 2007

Simultaneous XMM-Newton of the flare star

Hamburger Sternwarte, Universität Hamburg, Gojenbergsweg 112, 21029 Hamburg, Germany
Received 11 August 2006 / Accepted 23 January 2007

AKA 468, 221-221 (2007)
DOI: 10.1051/0004-6461/20062220
© ESO 2007

Simultaneous XMM-Newton of the flare star

Hamburger Sternwarte, Universität Hamburg, Gojenbergsweg 112, 21029 Hamburg, Germany
Received 11 August 2006 / Accepted 23 January 2007

Simultaneous XMM-Newton of the flare star

Hamburger Sternwarte, Universität Hamburg, Gojenbergsweg 112, 21029 Hamburg, Germany
Received 11 August 2006 / Accepted 23 January 2007

Simultaneous XMM-Newton of the flare star

Mem. S.A.I. Vol. 75, 282
© SAI 2004

Magnetic field variat

Multiwavelength ob

C. Lielke¹, A. Reiners^{1,2}

¹ Hamburger Sternwarte, Gojenbergsweg 112, 21029 Hamburg, Germany
² Georg-August-Universität Göttingen, List 2-37077 Göttingen, Germany
e-mail: c.lielke@hs.uni-hamburg.de

1. Introduction

Abstract. The M5.5 dwarf CN Leo has been observed with VLT/UVES on three nights in May 2004 deduced from FeI lines in the UVES spectra by all instruments. Time-resolved spectroscopy and emission measure of the coronal flux derived during the flare from the O IV triple behavior of chromospheric and transition region chromospheric emission lines are accompanied level. The Balmer lines show strong broadening and emission measure during the flare.

Key words. Stars: activity – Stars: magnetic individual: CN Leo – X-rays: stars

1. Introduction

In active M dwarfs stellar activity indicators like chromospheric H α emission and coronal X-ray emission can reach values orders of magnitude higher than observed in the Sun. Substantial variability can be seen in all wavelength bands, and frequent and strong flaring with flux increases by factors up to several hundreds is widespread among these objects (e.g. Gidel et al. 2002; Stiller et al. 2006). The origin of these flare events is usually described to magnetic reconnection, with the underlying magnetic fields of active M dwarfs reaching up

Based on observations collected at the European Southern Observatory, Paranal, Chile, 07/12-01/01/10 and on observations obtained with XMM-Newton, an ESA science mission with instruments and contributions directly funded by ESA Member States and NASA.

* Main-Content International Ongoing Follow-up.

Based on observations collected at the European Southern Observatory, Paranal, Chile, 07/12-01/01/10 and on observations obtained with XMM-Newton, an ESA science mission with instruments and contributions directly funded by ESA Member States and NASA.

Based on observations collected at the European Southern Observatory, Paranal, Chile, 07/12-01/01/10 and on observations obtained with XMM-Newton, an ESA science mission with instruments and contributions directly funded by ESA Member States and NASA.

Based on observations collected at the European Southern Observatory, Paranal, Chile, 07/12-01/01/10 and on observations obtained with XMM-Newton, an ESA science mission with instruments and contributions directly funded by ESA Member States and NASA.

Based on observations collected at the European Southern Observatory, Paranal, Chile, 07/12-01/01/10 and on observations obtained with XMM-Newton, an ESA science mission with instruments and contributions directly funded by ESA Member States and NASA.

Based on observations collected at the European Southern Observatory, Paranal, Chile, 07/12-01/01/10 and on observations obtained with XMM-Newton, an ESA science mission with instruments and contributions directly funded by ESA Member States and NASA.

Based on observations collected at the European Southern Observatory, Paranal, Chile, 07/12-01/01/10 and on observations obtained with XMM-Newton, an ESA science mission with instruments and contributions directly funded by ESA Member States and NASA.

Based on observations collected at the European Southern Observatory, Paranal, Chile, 07/12-01/01/10 and on observations obtained with XMM-Newton, an ESA science mission with instruments and contributions directly funded by ESA Member States and NASA.

Based on observations collected at the European Southern Observatory, Paranal, Chile, 07/12-01/01/10 and on observations obtained with XMM-Newton, an ESA science mission with instruments and contributions directly funded by ESA Member States and NASA.

Based on observations collected at the European Southern Observatory, Paranal, Chile, 07/12-01/01/10 and on observations obtained with XMM-Newton, an ESA science mission with instruments and contributions directly funded by ESA Member States and NASA.

Based on observations collected at the European Southern Observatory, Paranal, Chile, 07/12-01/01/10 and on observations obtained with XMM-Newton, an ESA science mission with instruments and contributions directly funded by ESA Member States and NASA.

Based on observations collected at the European Southern Observatory, Paranal, Chile, 07/12-01/01/10 and on observations obtained with XMM-Newton, an ESA science mission with instruments and contributions directly funded by ESA Member States and NASA.

Based on observations collected at the European Southern Observatory, Paranal, Chile, 07/12-01/01/10 and on observations obtained with XMM-Newton, an ESA science mission with instruments and contributions directly funded by ESA Member States and NASA.

Based on observations collected at the European Southern Observatory, Paranal, Chile, 07/12-01/01/10 and on observations obtained with XMM-Newton, an ESA science mission with instruments and contributions directly funded by ESA Member States and NASA.

Based on observations collected at the European Southern Observatory, Paranal, Chile, 07/12-01/01/10 and on observations obtained with XMM-Newton, an ESA science mission with instruments and contributions directly funded by ESA Member States and NASA.

Based on observations collected at the European Southern Observatory, Paranal, Chile, 07/12-01/01/10 and on observations obtained with XMM-Newton, an ESA science mission with instruments and contributions directly funded by ESA Member States and NASA.

Based on observations collected at the European Southern Observatory, Paranal, Chile, 07/12-01/01/10 and on observations obtained with XMM-Newton, an ESA science mission with instruments and contributions directly funded by ESA Member States and NASA.

Based on observations collected at the European Southern Observatory, Paranal, Chile, 07/12-01/01/10 and on observations obtained with XMM-Newton, an ESA science mission with instruments and contributions directly funded by ESA Member States and NASA.

Based on observations collected at the European Southern Observatory, Paranal, Chile, 07/12-01/01/10 and on observations obtained with XMM-Newton, an ESA science mission with instruments and contributions directly funded by ESA Member States and NASA.

Based on observations collected at the European Southern Observatory, Paranal, Chile, 07/12-01/01/10 and on observations obtained with XMM-Newton, an ESA science mission with instruments and contributions directly funded by ESA Member States and NASA.

Based on observations collected at the European Southern Observatory, Paranal, Chile, 07/12-01/01/10 and on observations obtained with XMM-Newton, an ESA science mission with instruments and contributions directly funded by ESA Member States and NASA.

Based on observations collected at the European Southern Observatory, Paranal, Chile, 07/12-01/01/10 and on observations obtained with XMM-Newton, an ESA science mission with instruments and contributions directly funded by ESA Member States and NASA.

Based on observations collected at the European Southern Observatory, Paranal, Chile, 07/12-01/01/10 and on observations obtained with XMM-Newton, an ESA science mission with instruments and contributions directly funded by ESA Member States and NASA.

Based on observations collected at the European Southern Observatory, Paranal, Chile, 07/12-01/01/10 and on observations obtained with XMM-Newton, an ESA science mission with instruments and contributions directly funded by ESA Member States and NASA.

Based on observations collected at the European Southern Observatory, Paranal, Chile, 07/12-01/01/10 and on observations obtained with XMM-Newton, an ESA science mission with instruments and contributions directly funded by ESA Member States and NASA.

Based on observations collected at the European Southern Observatory, Paranal, Chile, 07/12-01/01/10 and on observations obtained with XMM-Newton, an ESA science mission with instruments and contributions directly funded by ESA Member States and NASA.

Based on observations collected at the European Southern Observatory, Paranal, Chile, 07/12-01/01/10 and on observations obtained with XMM-Newton, an ESA science mission with instruments and contributions directly funded by ESA Member States and NASA.

Based on observations collected at the European Southern Observatory, Paranal, Chile, 07/12-01/01/10 and on observations obtained with XMM-Newton, an ESA science mission with instruments and contributions directly funded by ESA Member States and NASA.

Based on observations collected at the European Southern Observatory, Paranal, Chile, 07/12-01/01/10 and on observations obtained with XMM-Newton, an ESA science mission with instruments and contributions directly funded by ESA Member States and NASA.

Based on observations collected at the European Southern Observatory, Paranal, Chile, 07/12-01/01/10 and on observations obtained with XMM-Newton, an ESA science mission with instruments and contributions directly funded by ESA Member States and NASA.

Based on observations collected at the European Southern Observatory, Paranal, Chile, 07/12-01/01/10 and on observations obtained with XMM-Newton, an ESA science mission with instruments and contributions directly funded by ESA Member States and NASA.

Based on observations collected at the European Southern Observatory, Paranal, Chile, 07/12-01/01/10 and on observations obtained with XMM-Newton, an ESA science mission with instruments and contributions directly funded by ESA Member States and NASA.

Based on observations collected at the European Southern Observatory, Paranal, Chile, 07/12-01/01/10 and on observations obtained with XMM-Newton, an ESA science mission with instruments and contributions directly funded by ESA Member States and NASA.

Based on observations collected at the European Southern Observatory, Paranal, Chile, 07/12-01/01/10 and on observations obtained with XMM-Newton, an ESA science mission with instruments and contributions directly funded by ESA Member States and NASA.

Based on observations collected at the European Southern Observatory, Paranal, Chile, 07/12-01/01/10 and on observations obtained with XMM-Newton, an ESA science mission with instruments and contributions directly funded by ESA Member States and NASA.

Based on observations collected at the European Southern Observatory, Paranal, Chile, 07/12-01/01/10 and on observations obtained with XMM-Newton, an ESA science mission with instruments and contributions directly funded by ESA Member States and NASA.

Based on observations collected at the European Southern Observatory, Paranal, Chile, 07/12-01/01/10 and on observations obtained with XMM-Newton, an ESA science mission with instruments and contributions directly funded by ESA Member States and NASA.

Based on observations collected at the European Southern Observatory, Paranal, Chile, 07/12-01/01/10 and on observations obtained with XMM-Newton, an ESA science mission with instruments and contributions directly funded by ESA Member States and NASA.

Based on observations collected at the European Southern Observatory, Paranal, Chile, 07/12-01/01/10 and on observations obtained with XMM-Newton, an ESA science mission with instruments and contributions directly funded by ESA Member States and NASA.

Based on observations collected at the European Southern Observatory, Paranal, Chile, 07/12-01/01/10 and on observations obtained with XMM-Newton, an ESA science mission with instruments and contributions directly funded by ESA Member States and NASA.

Based on observations collected at the European Southern Observatory, Paranal, Chile, 07/12-01/01/10 and on observations obtained with XMM-Newton, an ESA science mission with instruments and contributions directly funded by ESA Member States and NASA.

Based on observations collected at the European Southern Observatory, Paranal, Chile, 07/12-01/01/10 and on observations obtained with XMM-Newton, an ESA science mission with instruments and contributions directly funded by ESA Member States and NASA.

Based on observations collected at the European Southern Observatory, Paranal, Chile, 07/12-01/01/10 and on observations obtained with XMM-Newton, an ESA science mission with instruments and contributions directly funded by ESA Member States and NASA.

Based on observations collected at the European Southern Observatory, Paranal, Chile, 07/12-01/01/10 and on observations obtained with XMM-Newton, an ESA science mission with instruments and contributions directly funded by ESA Member States and NASA.

Based on observations collected at the European Southern Observatory, Paranal, Chile, 07/12-01/01/10 and on observations obtained with XMM-Newton, an ESA science mission with instruments and contributions directly funded by ESA Member States and NASA.

Based on observations collected at the European Southern Observatory, Paranal, Chile, 07/12-01/01/10 and on observations obtained with XMM-Newton, an ESA science mission with instruments and contributions directly funded by ESA Member States and NASA.

Based on observations collected at the European Southern Observatory, Paranal, Chile, 07/12-01/01/10 and on observations obtained with XMM-Newton, an ESA science mission with instruments and contributions directly funded by ESA Member States and NASA.

Based on observations collected at the European Southern Observatory, Paranal, Chile, 07/12-01/01/10 and on observations obtained with XMM-Newton, an ESA science mission with instruments and contributions directly funded by ESA Member States and NASA.

Based on observations collected at the European Southern Observatory, Paranal, Chile, 07/12-01/01/10 and on observations obtained with XMM-Newton, an ESA science mission with instruments and contributions directly funded by ESA Member States and NASA.

Based on observations collected at the European Southern Observatory, Paranal, Chile, 07/12-01/01/10 and on observations obtained with XMM-Newton, an ESA science mission with instruments and contributions directly funded by ESA Member States and NASA.

Based on observations collected at the European Southern Observatory, Paranal, Chile, 07/12-01/01/10 and on observations obtained with XMM-Newton, an ESA science mission with instruments and contributions directly funded by ESA Member States and NASA.

Based on observations collected at the European Southern Observatory, Paranal, Chile, 07/12-01/01/10 and on observations obtained with XMM-Newton, an ESA science mission with instruments and contributions directly funded by ESA Member States and NASA.

Based on observations collected at the European Southern Observatory, Paranal, Chile, 07/12-01/01/10 and on observations obtained with XMM-Newton, an ESA science mission with instruments and contributions directly funded by ESA Member States and NASA.

Based on observations collected at the European Southern Observatory, Paranal, Chile, 07/12-01/01/10 and on observations obtained with XMM-Newton, an ESA science mission with instruments and contributions directly funded by ESA Member States and NASA.

Based on observations collected at the European Southern Observatory, Paranal, Chile, 07/12-01/01/10 and on observations obtained with XMM-Newton, an ESA science mission with instruments and contributions directly funded by ESA Member States and NASA.

Based on observations collected at the European Southern Observatory, Paranal, Chile, 07/12-01/01/10 and on observations obtained with XMM-Newton, an ESA science mission with instruments and contributions directly funded by ESA Member States and NASA.

Based on observations collected at the European Southern Observatory, Paranal, Chile, 07/12-01/01/10 and on observations obtained with XMM-Newton, an ESA science mission with instruments and contributions directly funded by ESA Member States and NASA.

Based on observations collected at the European Southern Observatory, Paranal, Chile, 07/12-01/01/10 and on observations obtained with XMM-Newton, an ESA science mission with instruments and contributions directly funded by ESA Member States and NASA.

Based on observations collected at the European Southern Observatory, Paranal, Chile, 07/12-01/01/10 and on observations obtained with XMM-Newton, an ESA science mission with instruments and contributions directly funded by ESA Member States and NASA.

Based on observations collected at the European Southern Observatory, Paranal, Chile, 07/12-01/01/10 and on observations obtained with XMM-Newton, an ESA science mission with instruments and contributions directly funded by ESA Member States and NASA.

Based on observations collected at the European Southern Observatory, Paranal, Chile, 07/12-01/01/10 and on observations obtained with XMM-Newton, an ESA science mission with instruments and contributions directly funded by ESA Member States and NASA.

Based on observations collected at the European Southern Observatory, Paranal, Chile, 07/12-01/01/10 and on observations obtained with XMM-Newton, an ESA science mission with instruments and contributions directly funded by ESA Member States and NASA.

Based on observations collected at the European Southern Observatory, Paranal, Chile, 07/12-01/01/10 and on observations obtained with XMM-Newton, an ESA science mission with instruments and contributions directly funded by ESA Member States and NASA.

Based on observations collected at the European Southern Observatory, Paranal, Chile, 07/12-01/01/10 and on observations obtained with XMM-Newton, an ESA science mission with instruments and contributions directly funded by ESA Member States and NASA.

Based on observations collected at the European Southern Observatory, Paranal, Chile, 07/12-01/01/10 and on observations obtained with XMM-Newton, an ESA science mission with instruments and contributions directly funded by ESA Member States and NASA.

Based on observations collected at the European Southern Observatory, Paranal, Chile, 07/12-01/01/10 and on observations obtained with XMM-Newton, an ESA science mission with instruments and contributions directly funded by ESA Member States and NASA.

Based on observations collected at the European Southern Observatory, Paranal, Chile, 07/12-01/01/10 and on observations obtained with XMM-Newton, an ESA science mission with instruments and contributions directly funded by ESA Member States and NASA.

Based on observations collected at the European Southern Observatory, Paranal, Chile, 07/12-01/01/10 and on observations obtained with XMM-Newton, an ESA science mission with instruments and contributions directly funded by ESA Member States and NASA.

Based on observations collected at the European Southern Observatory, Paranal, Chile, 07/12-01/01/10 and on observations obtained with XMM-Newton, an ESA science mission with instruments and contributions directly funded by ESA Member States and NASA.

Based on observations collected at the European Southern Observatory, Paranal, Chile, 07/12-01/01/10 and on observations obtained with XMM-Newton, an ESA science mission with instruments and contributions directly funded by ESA Member States and NASA.

Based on observations collected at the European Southern Observatory, Paranal, Chile, 07/12-01/01/10 and on observations obtained with XMM-Newton, an ESA science mission with instruments and contributions directly funded by ESA Member States and NASA.

Based on observations collected at the European Southern Observatory, Paranal, Chile, 07/12-01/01/10 and on observations obtained with XMM-Newton, an ESA science mission with instruments and contributions directly funded by ESA Member States and NASA.

Based on observations collected at the European Southern Observatory, Paranal, Chile, 07/12-01/01/10 and on observations obtained with XMM-Newton, an ESA science mission with instruments and contributions directly funded by ESA Member States and NASA.

Based on observations collected at the European Southern Observatory, Paranal, Chile, 07/12-01/01/10 and on observations obtained with XMM-Newton, an ESA science mission with instruments and contributions directly funded by ESA Member States and NASA.

Based on observations collected at the European Southern Observatory, Paranal, Chile, 07/12-01/01/10 and on observations obtained with XMM-Newton, an ESA science mission with instruments and contributions directly funded by ESA Member States and NASA.

Based on observations collected at the European Southern Observatory, Paranal, Chile, 07/12-01/01/10 and on observations obtained with XMM-Newton, an ESA science mission with instruments and contributions directly funded by ESA Member States and NASA.

Based on observations collected at the European Southern Observatory, Paranal, Chile, 07/12-01/01/10 and on observations obtained with XMM-Newton, an ESA science mission with instruments and contributions directly funded by ESA Member States and NASA.